analytical chemistry

Article

pubs.acs.org/ac

Direct Raman Spectroscopic Measurements of Biological Nitrogen Fixation under Natural Conditions: An Analytical Approach for Studying Nitrogenase Activity

Tobias Jochum,[†] Agnes Fastnacht,[‡] Susan E. Trumbore,[‡] Jürgen Popp,[†,§] and Torsten Frosch*[,†,§]

[†]Leibniz Institute of Photonic Technology, 07745 Jena, Germany

[‡]Max Planck Institute for Biogeochemistry, 07745 Jena, Germany

[§]Institute of Physical Chemistry and Abbe Center of Photonics, 07745 Jena, Germany

Supporting Information

ABSTRACT: Biological N_2 fixation is a major input of bioavailable nitrogen, which represents the most frequent factor limiting the agricultural production throughout the world. Especially, the symbiotic association between legumes and *Rhizobium* bacteria can provide substantial amounts of nitrogen (N) and reduce the need for industrial fertilizers. Despite its importance in the global N cycle, rates of biological nitrogen fixation have proven difficult to quantify. In this work, we propose and demonstrate a simple analytical approach to measure biological N_2 fixation rates directly without a proxy or isotopic labeling. We determined a mean N_2 fixation rate of 78 ± 5 μmol N_2 (g dry weight nodule)$^{-1}$ h^{-1} of a *Medicago sativa*−*Rhizobium* consortium by continuously analyzing the amount of atmospheric N_2 in static environmental chambers with Raman gas spectroscopy. By simultaneously analyzing the CO_2 uptake and photosynthetic plant activity, we think that a minimum CO_2 mixing ratio might be needed for natural N_2 fixation and only used the time interval above this minimum CO_2 mixing ratio for N_2 fixation rate calculations. The proposed approach relies only on noninvasive measurements of the gas phase and, given its simplicity, indicates the potential to estimate biological nitrogen fixation of legume symbioses not only in laboratory experiments. The same methods can presumably also be used to detect N_2 fluxes by denitrification from ecosystems to the atmosphere.

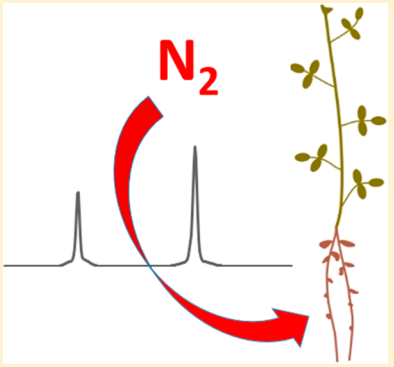

Nitrogen is an essential element for the synthesis of proteins and thus for sustaining life.[1] In the form of dinitrogen gas (N_2), it is abundantly available in the earth's atmosphere, but most organisms are unable to metabolize it.[2] Instead, N_2 needs to be converted to its hydrogenated product ammonia (NH_3) to become usable.[3] This process is known as nitrogen fixation[4] and represents a crucial step in the biogeochemical nitrogen cycle.[5] Only diazotrophs fix N_2 biologically[6] using a nitrogenase enzyme system,[7] which carries out the metabolically expensive reduction of N_2 to ammonia (NH_3) via

$$N_2 + 8e^- + 16ATP + 8H^+ \rightarrow 2NH_3 + H_2 + 16ADP + 16P_i \quad (1)$$

(P_i, inorganic phosphate). The nitrogenase activity is influenced by a variety of environmental factors including moisture, light level, temperature, trace metal availability, or the nitrogen to phosphorus ratio.[8] Despite its importance, environmental and physiological controls of biological nitrogen fixation (BNF) rates are not completely understood.[9] Quantification of N_2 fixation rates at the field level or in real time is difficult,[10] particularly because of the high natural background of N_2.[11] Further progress in technical instrumentation and analytical methods is needed to understand principal factors regulating N_2 fixation and to facilitate its management for the benefit of the environment or agricultural productivity. In this work, a novel analytical approach based on Raman gas spectroscopy is proposed, which enables the determination of biological nitrogen fixation rates without requiring a proxy or an exchange of the natural ecosystem atmosphere. Given its simplicity, the proposed method indicates the potential to open up a new avenue of nitrogen fixation research.

Existing direct methods for quantifying biological nitrogen fixation in plants and soils vary widely. For plants, the N difference method compares total N in N-fixing and non-N-fixing species. However, the N-fixing and the control plants may differ in their capacity to use soil nitrogen if their root morphology or rooting depths differ.[12] If soil mineral N has a different isotopic signature compared to atmospheric N, a mass balance approach can be used to estimate the fraction of plant N from each source (^{15}N natural abundance). This technique is reliable, but typically destructive, and integrates fluxes over long experimental times. Finally, another direct method to estimate BNF rates uses ^{15}N tracer, where N-fixing systems are

Received: August 9, 2016
Accepted: December 12, 2016
Published: December 22, 2016

DOI: 10.1021/acs.analchem.6b03101
Anal. Chem. 2017, 89, 1117−1122

incubated with isotopically enriched $^{15}N_2$ gas followed by the analysis of assimilated ^{15}N in plants or bacteria.[13] The ^{15}N incubation methodology is a highly sensitive and direct measure of nitrogen fixation, but destructive, integrates over time scales of hours (i.e., not real time), and is additionally limited to systems that can be enclosed in a ^{15}N atmosphere. This restricts the ^{15}N incubation method to small-scale laboratory experiments over short time frames.

Other methods to measure N_2 fixation rely on the detection of reaction intermediates or N_2 fixation inhibition. Nitrogenase activity can be measured indirectly by quantifying hydrogen evolution, because H_2 is an obligate byproduct of N_2 fixation (see eq 1), e.g., in legume nodules.[14] But H_2 represents only a portion of the total electron flux through nitrogenase. This necessitates the incubation of investigated nodules in a N_2-free atmosphere to measure the total nitrogenase activity,[15] which is not suitable for many field-based applications. Additionally, the hydrogen evolution technique cannot be applied if hydrogenase enzymes are active in the nodules, which scavenge H_2 produced by the nitrogenase.[16] Another indirect, frequently used method to assess BNF is the acetylene reduction assay (ARA),[17] as it is a simple, relatively inexpensive, and sensitive tool[18] for short-term monitoring of the nitrogenase activity.[19] Acetylene (C_2H_2) competitively inhibits N_2 fixation[20] and is converted to ethylene (C_2H_4) by the nitrogenase enzyme.[21] However, several difficulties arise when ARA is used in quantitative studies, e.g., for estimating the total N_2 fixation of a *Rhizobium*−Leguminosae symbiosis.[22] Acetylene could induce a decline in nitrogenase activity in some legume species as well as in respiration, if N_2 is replaced with argon or helium.[23] Further, the conversion ratio of reduced C_2H_2 to fixed N_2 is highly variable[24] and often differs from theoretical biochemical calculations.[25] This is especially the case when alternative vanadium- or iron-type nitrogenases are active besides the canonical molybdenum-type nitrogenase.[26]

In this work, we propose and demonstrate a novel approach for measuring biological nitrogen fixation by plant−diazotrophic bacteria symbioses. The nitrogenase activity is quantified by continuous spectral monitoring of the gaseous $^{14}N_2$ concentration in environmental chambers housing alfalfa plants (*Medicago sativa* L.). Here, the amount of N_2 in the chamber headspace is monitored by Raman gas spectroscopy.[27] This approach offers several benefits; it is sensitive, nonconsumptive, does not require nonfixing reference plants, additionally injected gases, or isotopic labeling, and allows for continuous detection of the nitrogen fixation dynamics at ambient N_2 levels. We report on the first biological nitrogen fixation rate estimates derived by optical spectroscopy of N_2 and discuss potential limitations and expansions of the presented method as a prelude to future investigations.

MATERIALS AND METHODS

Plant Growth. When it comes to agricultural nitrogen fixation inputs, most attention is directed toward legumes, because of their proven ability to fix N_2 symbiotically in tropical and temperate environments.[28] The plant we selected, the perennial legume *M. sativa*, takes a large fraction of its nitrogen from N_2 fixation (up to 100% when grown in a mixture with grasses).[29] *M. sativa* seed (Feldsaaten Freudenberger, Germany) was grown in plastic pots on N- and C-free quartz sand under controlled greenhouse conditions of 25/20 ± 1 °C (day/night, each 12 h). During cloudy or rainy days, natural sunlight was supplemented with sodium vapor lamps (400 W Gro-Lux, Osram Sylvania Ltd., U.S.A.) providing a minimum photosynthetic photon flux density (PPFD) of 400−500 μmol m^{-2} s^{-1}. Plants were inoculated with a commercial *Rhizobium* inoculant (RhizoFix, Feldsaaten Freudenberger, Germany) according to the manufacturers' instructions. The pots were fertilized weekly with a Hoagland solution[30] lacking ammonium nitrate (NH_4NO_3), forcing the plants to rely on symbiotic N_2 fixation as a source for nitrogen.[31] The inoculation led to effective nodulation, while noninoculated controls died due to N starvation. After the N_2 fixation measurements, nodules were detached and dried to a constant weight at 60 °C. Biological N_2 fixation rates were calculated on a nodule dry weight basis.

Experimental Design. N_2 fixation was measured in a laboratory chamber system with an internal volume of 3.0 L (Figure 1). The cylindrical plant chamber consists of acrylic glass and is connected to a pump and the Raman gas analyzer via polyurethane tubes. Different chamber volumes or geometries are also feasible, as long as they provide enough space for internal sensors and tube ports. Before the gas measurements, the quartz sand was carefully removed from the plants. In each measurement run (samples 1−5) several alfalfa plants were grouped and measured together. After introducing the undisturbed alfalfa plants including roots and nodules into the chamber, the headspace air was monitored continuously in a static mode. By using whole plants in just one compartment, the total gas exchange of the plant can be quantified. Elevated CO_2 levels are avoided because of the active leaf photosynthesis. Thus, a potential physiological influence of enhanced CO_2 levels on the specific nitrogenase activity of legume nodules,[32] which is still under discussion,[33,34] does not affect our measurements. However, significantly decreased CO_2 concentrations, and thus low photosynthetic activity, seem to have an effect on biological N_2 fixation. We considered this by incorporating a lower CO_2 threshold for BNF calculation; see the discussion in the following section.

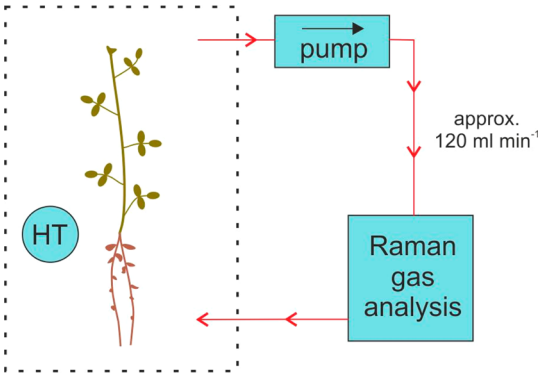

Figure 1. Schematic sketch of the experimental setup for continuous N_2 monitoring. Gases from the plant chamber are pumped to the Raman gas analyzer, measured, and returned to the chamber without change or consumption. The air humidity and temperature are recorded by an internal sensor (HT).

A diaphragm pump circulated air with a constant flow rate of ~120 mL min^{-1} from the plant compartment to the Raman gas analyzer and back. To measure the partial pressure of water vapor, a humidity and temperature sensor (model UFT75-AT, Sensor-Tec, Germany) was installed. As ambient air was used as initial plant atmosphere, no equilibration time for homogeneous gas mixing within the system is necessary and possible changes of the gas composition can be directly observed after

DOI: 10.1021/acs.analchem.6b03101
Anal. Chem. 2017, 89, 1117−1122

closing the chamber. Separate test measurements showed no detectable inherent N_2 leakage into the chamber system within typical experimental times of up to several hours. This illustrates on the one hand the airtight chamber design. On the other hand, N_2 leakage is additionally hindered by very low concentration gradients between the natural atmospheric background and the N_2 level inside the chamber system. The plant chamber was illuminated by a horticulture LED lamp (model M30, SANlight, Austria) providing a photosynthetic photon flux density of ∼150 μmol m^{-2} s^{-1}. All experiments were performed in a controlled growth cabinet at ∼25 °C.

For testing our method, we used five individual measurements. After introducing the complete plant with root and attached nodules, the chamber was closed and the headspace gases continuously analyzed by Raman gas spectroscopy. A spectrum was recorded every 10 s.

Raman Gas Analysis. Although gas chromatography (GC) coupled to various detector types is a very sensitive technique to quantify N_2,[35] it does not provide as high temporal resolution as Raman gas spectroscopy and also operates sample destructively. In most applications, N_2 exchange rates cannot be measured by GC techniques due to the high natural N_2 background concentration.[36] Thus, we applied Raman gas spectroscopy[37−39] for monitoring biological N_2 fixation. In Raman gas spectroscopy, the scattered light from gas molecules interacting with a laser contains information about their molecular structure and abundance.[40,41] Hence, analyzing this scattered light enables molecule identification and quantification.[42−45] The in-house built Raman gas analyzer (λ_{laser} = 650 nm, P_{laser} = 50 mW, spectral resolution ∼50 cm^{-1}), which uses an optical cavity to enhance the laser intensity, has been described previously.[46−49] Briefly, mixing ratios are measured by analyzing the Raman light originating from gas molecules passing the optical cavity (volume ∼4 cm^3) at atmospheric pressure. For the investigated gases, the instrument provides a measurement range from ∼200 ppm (limit of detection, LOD) up to 100%. Investigated gases do not undergo any pretreatment and are not altered during the measurement procedure. Internal sensors record the current gas pressure and temperature in the cavity, which enables the calculation of partial pressures and absolute molecule numbers of the analyzed gases.

The instrument was calibrated with spectra of pure reference gases (N_2, O_2, and CO_2, Linde, Germany), which were measured individually and built the basis set for the data analysis. First, the spectral background was corrected by subtraction of a spectrum of the Raman-inactive noble gas argon. Second, the measured spectra were normalized by the current intracavity pressure and laser intensity. In the third step, a multiple linear regression was applied to predict weighting coefficients for N_2, O_2, and CO_2. Experimental spectra comprising a mixture of spectral features can then be expressed as a sum of the basis set spectra, where the weighting coefficients of each basis spectrum are proportional to the mixing ratios of that species (Figure S1). This strategy[50] allows for simultaneous quantification of several constituents in a gas mixture while minimizing cross interferences.[51] The robustness of this spectral data analysis was tested with reference gases comprising N_2, O_2, CO_2, and Ar at various mixing ratios close to experimental compositions. Reference gases were created using mass flow controllers (model GF80, Brooks Instrument, U.S.A.), which were calibrated using a primary standard air flow calibrator (model Gilibrator II, Sensidyne, U.S.A.). From these test measurements, a relative accuracy of about 1% was determined for the range of relevant N_2 mixing ratios (v/v), i.e., mixing ratios between (70 ± 0.7)% and (80 ± 0.8)% (Figure S2). The relative accuracy of O_2 was also 1% for mixing ratios (v/v) between 16% and 23%. Additional tests comparing measured CO_2 mixing ratios of prepared reference gases by the Raman instrument with a nondispersive infrared (NDIR) analyzer (model LI-840A, LI-COR Biosciences, U.S.A.) indicated a relative accuracy of the CO_2 mixing ratio of ∼1% for CO_2 mixing ratios from 0 to 1500 ppm (v/v).

Water Vapor and Absolute Gas Quantity Calculation. In contrast to absorption spectroscopy techniques, water vapor yields only a weak Raman signal, which does not interfere with the main spectral features of N_2, O_2, and CO_2 (Q branches at 2331 and 1556 cm^{-1} for N_2 and O_2, respectively, as well as the Fermi dyad of CO_2 at 1388 and 1285 cm^{-1}). Thus, no water vapor correction was necessary, which was experimentally confirmed in separate tests. However, we monitored water vapor levels to avoid measurements under dry conditions, which might affect nitrogen fixation. The partial pressure of water vapor, p_{H_2O}, was quantified using the Antoine equation. The relative humidity ϕ in the environmental chamber is measured by the humidity sensor and converted to the water vapor partial pressure as

$$\log_{10} p_{H_2O}{}^{eq} = A - \frac{B}{C + T} \tag{2}$$

with temperature T in Celsius, $p_{H_2O}{}^{eq}$ the equilibrium water vapor pressure (mmHg) at that temperature, and the coefficients A = 8.05573, B = 1723.6425, and C = 233.08.[52] The current water vapor partial pressure p_{H_2O} is then given by the product of the relative humidity and the equilibrium water vapor pressure:

$$p_{H_2O} = \phi p_{H_2O}{}^{eq} \tag{3}$$

Determined p_{H_2O} values were validated in separate test measurements beforehand using the NDIR analyzer, indicating a relative accuracy for p_{H_2O} of ∼1.8%.

The applied gas analysis strategy provides measurement data in units of the dimensionless volume mixing ratio χ_i (in 10^{-6} = ppm) of the corresponding gas species i. But for the calculation of release or consumption rates J_i (e.g., in mol $g_{dw}{}^{-1}$ s^{-1} or g $g_{dw}{}^{-1}$ s^{-1}), absolute quantities such as the amount of substance (in moles) or the mass (in grams) have to be used. Following ideal gas laws and Dalton's law, we determined the amount of substance n_i of the gas species i by

$$n_i = \frac{\chi_i PV}{RT} \tag{4}$$

with χ_i being the volume mixing ratio, P the total barometric pressure (hPa), V the system volume (m^3), R the universal gas constant (8.314 × 10^{-2} m^3 hPa K^{-1} mol^{-1}), and T the current air temperature (K) of the chamber headspace. By multiplication with the molar mass M_i (g mol^{-1}) of the corresponding gas species i (28.014 for N_2, 31.999 for O_2, and 44.010 for CO_2), the mass m_i was calculated as

$$m_i = n_i M_i \tag{5}$$

The calculated mixing ratios refer to humid air, as the total barometric pressure P includes water vapor. Using absolute quantities instead of volume mixing ratios was of particular importance, as varying water vapor levels during our experi-

DOI: 10.1021/acs.analchem.6b03101
Anal. Chem. 2017, 89, 1117−1122

ments caused a significant dilution of the other gases. Relative humidity levels of up to 85−95% were observed during the chamber measurements, which correspond to water vapor partial pressures of almost 30 hPa.

RESULTS AND DISCUSSION

For calculation of the N_2 fixation rates, we first determined what time interval was suitable, based on our monitoring of plant photosynthetic activity and CO_2 uptake. Then, a linear regression (ANOVA, analysis of variance) was performed onto the temporal evolution of n_{N2}, the amount of N_2 in the chamber. This is exemplarily illustrated in Figure 2, which

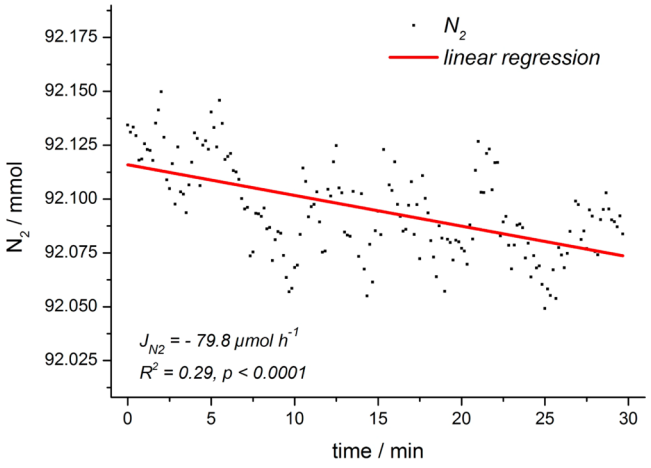

Figure 2. N_2 fixation rate calculation. The slope of a linear regression onto the amount of N_2 in the chamber atmosphere yields the N_2 fixation rate (μmol h^{-1}). The length of the respective time interval is defined by the CO_2 level. Data from sample 5 is depicted exemplarily for all alfalfa samples.

shows data from one of the analyzed *M. sativa* plants. The slope of the linear regression yields the biological N_2 fixation rate (here in micromoles of N_2 per hour). A negative rate means a decrease of N_2 in the chamber headspace, i.e., a biological uptake. The linear regression appears to be superimposed by a periodic fluctuation, which was most likely caused by a technical temperature feedback loop in the experimental setup. However, very low p values in each replicate measurement indicate a statistically significant correlation of the amount of N_2 in the headspace and time, i.e., biological N_2 fixation. Future technical improvements will help to decrease the temperature related fluctuations and, thus, the uncertainty of the linear approximation. Finally, the obtained rate was normalized to the nodule dry weight to account for differences between individual plants.

Photosynthetic Activity and CO_2 Uptake. N_2 fixation requires large amounts of energy (see eq 1), and thus rates of N_2 fixation may be affected by the rate of supply of C to mutualist bacteria by the plant. Although increasing leaf photosynthesis does not enhance the specific nitrogenase activity,[53] carbohydrate availability and especially bacterial carbon utilization within the nodule seem to play a role in regulating N_2 fixation.[54] Mobilization of reserve energy substrates by leguminous plants appears to have only a minor role, and readily available assimilates tend to be rapidly exhausted (within minutes).[55] Thus, when investigating N_2 fixation in legumes such as *M. sativa*, monitoring of the photosynthetic activity by analyzing current O_2 and CO_2 levels provides supplementary information about the relative effectiveness of biological N_2 fixation.

The five individual alfalfa plant replicates used in our experiments always showed net consumption of CO_2 and production of O_2, indicating that leaf net photosynthesis dominated root and nodule respiration fluxes (Table 1). The rate of net CO_2 consumption was initially generally constant (p values always less than 0.0001), until CO_2 mixing ratios had declined to ∼200−150 ppm (v/v), see Figure 3. Once CO_2

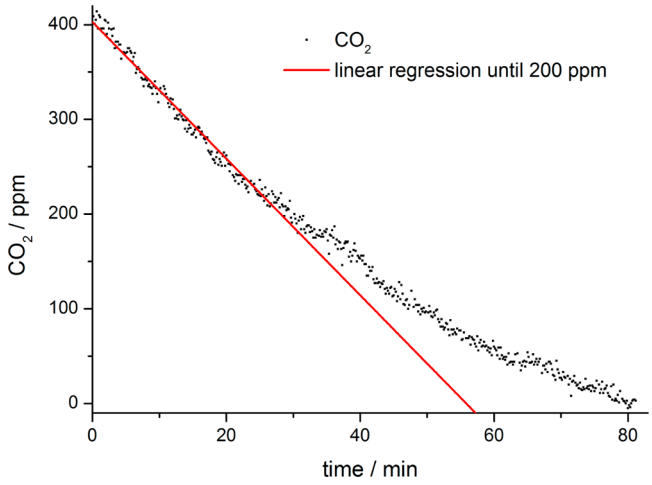

Figure 3. CO_2 uptake rate quantification. In general, CO_2 decreases linearly until a threshold of ∼150−200 ppm (v/v). Below this threshold a slower CO_2 decrease along with a reduced N_2 fixation was observed. Thus, we defined the time until ∼200 ppm (v/v) CO_2 is reached as the analysis time, the time interval for rate calculations of N_2, O_2, and CO_2. Data originates from sample 5.

levels dropped below ∼150 ppm (v/v), the rate of decline in CO_2 levels generally slowed, suggesting a change in the balance of photosynthesis and respiration and/or nodule CO_2 fixation mechanisms. In that phase, the rate of N_2 fixation also declined,

Table 1. Overview of the Nodule Biomass, Analysis Time, Total Plant CO_2 Uptake, and O_2 Release of the Individual Alfalfa Samples[a]

sample	nodule biomass (g)	analysis time (min)	plant CO_2 uptake (μmol CO_2 h^{-1})	O_2 release (μmol O_2 h^{-1})
1	0.38	148	14.7 (0.1)	14.1 (1.8)
2	0.52	54	14.4 (0.5)	12.5 (3.9)
3	0.40	202	27.1 (0.1)	14.4 (1.0)
4	0.53	77	33.5 (0.5)	29.7 (3.8)
5	1.04	30	79.8 (9.2)	53.6 (8.8)

[a]Data in parentheses shows the respective standard deviation. The gas rates indicate a dominant photosynthesis but also a significant contribution of nodule CO_2 fixation.

DOI: 10.1021/acs.analchem.6b03101
Anal. Chem. 2017, 89, 1117−1122

in a few cases even ceasing at low CO_2 concentrations. Although this behavior needs to be investigated in much more detail in future experiments, it suggests that very low CO_2 levels could limit symbiotic N_2 fixation.

To improve the comparability of measured N_2 fixation rates, we thus defined a time period based on the interval when CO_2 data declined at a constant rate, and the reported N_2 fixation rates were determined only during this time interval. We selected the time window from closing the chamber (ambient CO_2 levels) until reaching a CO_2 mixing ratio of ~200 ppm (v/v) for the calculation of the CO_2 uptake, O_2 release, and N_2 fixation rate. The time until this CO_2 threshold was reached, defined here as the analysis time, depended on the biomass (leaves, stem, roots, and nodules) inside the chamber and varied between 30 min (sample 5) and almost 3.5 h (sample 3). Figure 3 illustrates the time window selection and CO_2 rate quantification, exemplarily for sample 1.

CO_2 uptake rates of the total plant are strongly correlated with O_2 release rates (correlation coefficient of 0.97). However, O_2 release rates are generally lower than CO_2 uptake rates, suggesting that nodule CO_2 fixation contributes significantly to the total CO_2 consumption of the plant. Nodule CO_2 fixation is known to be tightly coupled to N_2 fixation, e.g., shown by the concomitant expression of phosphoenolpyruvate carboxylase (PEPC) in nodules and emerging nitrogenase activity.[56]

Biological N_2 Fixation Rates of *M. sativa*. Measured N_2 fixation rates (Table 2), normalized to the nodule biomass, ranged from 70 to 85 μmol N_2 (g dry weight nodule)$^{-1}$ h^{-1}, which corresponds to 47−57 mg N (g dry weight nodule)$^{-1}$ day^{-1}. These rates show no trend when compared to the nodule biomass, which indicates that in each measurement the majority of the nodules were actively fixing N_2. Further, the N_2 fixation rates do not correlate with the analysis time (correlation coefficient of 0.14). All determined rates are statistically significant ($p < 0.0001$); also the shortest analysis time of approximately half an hour yielded statistically robust data (Figure 2). Thus, the proposed N_2 fixation rate quantification is applicable to short-term measurements from 30 min up to several hours without introducing artifacts due to the static environmental chamber design.

Table 2. Raman Gas Spectroscopy Measurements of the N_2 Fixation of *M. sativa* Inoculated with Rhizobium[a]

	N_2 fixation	
sample	μmol N_2 g_{dw}^{-1} h^{-1}	mg N g_{dw}^{-1} day^{-1}
1	70 (15)	47 (10)
2	77 (16)	52 (11)
3	80 (9)	54 (6)
4	85 (18)	57 (12)
5	77 (9)	52 (6)
mean	78 (5)	52 (3)

[a]N_2 fixation rates are given in μmol N_2 (g dry weight nodule)$^{-1}$ h^{-1} (second column) and mg N (g dry weight nodule)$^{-1}$ day^{-1} (third column). Data in parentheses indicates the respective standard deviation.

The mean N_2 fixation rate yields 78 ± 5 μmol N_2 (g dry weight nodule)$^{-1}$ h^{-1} or 52 ± 3 mg N (g dry weight nodule)$^{-1}$ day^{-1}. These rates are within the range of reported values from biological nitrogen fixation studies with alfalfa and other legumes using the $^{15}N_2$ incubation[57,58] or the H_2 evolution[59] technique. A direct comparison of measured N_2 fixation rates by the Raman analyzer and another technique is not feasible, as to our best knowledge, there is no comparable method capable of simultaneously quantifying N_2 dynamics and photosynthetic activity directly, with similar temporal resolution and in view of the high N_2 background.

It should be noted that the proposed analytical approach quantifies the net N_2 decrease within a chamber atmosphere. While this method also indicates the potential to be applied in the field, or for plants together with soil, other processes, including relevant denitrification processes, may affect the measured flux, e.g., by releasing N_2. Thus, careful experimental design is crucial when applying the proposed method. In this study, we ensured this by inoculation with selected *Rhizobium* strains and the absence of soil microorganisms, which could have had a potential denitrification capability. To improve its applicability, the reported approach might also be compared directly to common techniques such as ^{15}N isotopic methods, ARA, or H_2 evolution. For this, measured nitrogen fixation estimates from the mentioned techniques and the Raman gas analysis should be determined for the same ecosystem and, in the case of ARA and H_2 evolution, a conversion factor derived. We envisage these comparison measurements in future experiments.

CONCLUSION

The analytical approach presented in this study using Raman gas spectroscopy and the natural atmospheric gas composition provides accurate determinations of the N_2 fixation capability of alfalfa plants that are comparable to results obtained using other techniques. As cavity Raman gas analyzers get more popular and offer high potential for miniaturization and cost reduction,[60] we envisage a significant decrease in analysis costs compared to standard methods using gas chromatography or N_2 isotopes. The proposed method simplifies and develops biological nitrogen fixation measurements by (1) using ambient N_2 as a direct indicator for BNF, (2) operating non-consumptive, (3) depending on no external isotopes or other gases, and (4) eliminating the need for nonfixing reference plants. Moreover, Raman gas spectroscopy has also the capability to measure O_2 and CO_2 dynamics simultaneously. This may open new research avenues in nitrogen cycling processes, such as interactions of N_2 fixation and respiration, photosynthesis, or CO_2 fixation mechanisms. Application of this novel technique will assist with the determination of biological nitrogen fixation rates and nitrogenase activity in legume−diazotroph symbioses and potentially increase the knowledge of the physiology of nitrogen fixation.

ASSOCIATED CONTENT

Supporting Information

The Supporting Information is available free of charge on the ACS Publications website at DOI: 10.1021/acs.analchem.6b03101.

Decomposition of a measured multigas spectrum into its components, and comparison of the N_2 reference mixing ratios and predicted mixing ratios by the Raman analysis (PDF)

AUTHOR INFORMATION

Corresponding Author

*E-mail: torsten.frosch@uni-jena.de; torsten.frosch@gmx.de.

DOI: 10.1021/acs.analchem.6b03101
Anal. Chem. 2017, 89, 1117−1122

ORCID
Torsten Frosch: 0000-0003-3358-8878

Notes

The authors declare no competing financial interest.

■ ACKNOWLEDGMENTS

The work has been funded by the Deutsche Forschungsgemeinschaft (DFG) CRC 1076 "AquaDiva". We thank Gabriela Pereyra from the Max Planck Institute for Biogeochemistry for her helpful advice in plant cultivation.

■ REFERENCES

(1) Canfield, D. E.; Glazer, A. N.; Falkowski, P. G. *Science* **2010**, *330*, 192−196.
(2) Cheng, Q. *J. Integr. Plant Biol.* **2008**, *50*, 786−798.
(3) Jia, H.-P.; Quadrelli, E. A. *Chem. Soc. Rev.* **2014**, *43*, 547−564.
(4) Cleveland, C. C.; Townsend, A. R.; Schimel, D. S.; Fisher, H.; Howarth, R. W.; Hedin, L. O.; Perakis, S. S.; Latty, E. F.; Von Fischer, J. C.; Elseroad, A.; Wasson, M. F. *Global Biogeochem Cy* **1999**, *13*, 623−645.
(5) Gruber, N.; Galloway, J. N. *Nature* **2008**, *451*, 293−296.
(6) Raymond, J.; Siefert, J. L.; Staples, C. R.; Blankenship, R. E. *Mol. Biol. Evol.* **2004**, *21*, 541−554.
(7) Hoffman, B. M.; Lukoyanov, D.; Yang, Z. Y.; Dean, D. R.; Seefeldt, L. C. *Chem. Rev.* **2014**, *114*, 4041−4062.
(8) Vitousek, P. M.; Cassman, K.; Cleveland, C.; Crews, T.; Field, C. B.; Grimm, N. B.; Howarth, R. W.; Marino, R.; Martinelli, L.; Rastetter, E. B.; Sprent, J. I. *Biogeochemistry* **2002**, *57*, 1−45.
(9) Unkovich, M. *New Phytol.* **2013**, *198*, 643−646.
(10) Cassar, N.; Bellenger, J. P.; Jackson, R. B.; Karr, J.; Barnett, B. A. *Oecologia* **2012**, *168*, 335−342.
(11) Davidson, E. A.; Seitzinger, S. *Ecol Appl.* **2006**, *16*, 2057−2063.
(12) Chalk, P. M. *Aust. J. Agric. Res.* **1998**, *49*, 303−316.
(13) Warembourg, F. R.; Montange, D.; Bardin, R. *Physiol. Plant.* **1982**, *56*, 46−55.
(14) Schubert, K. R.; Evans, H. J. *Proc. Natl. Acad. Sci. U. S. A.* **1976**, *73*, 1207−1211.
(15) Hunt, S.; Layzell, D. B. *Annu. Rev. Plant Physiol. Plant Mol. Biol.* **1993**, *44*, 483−511.
(16) Robson, R. L.; Postgate, J. R. *Annu. Rev. Microbiol.* **1980**, *34*, 183−207.
(17) Pinto-Tomas, A. A.; Anderson, M. A.; Suen, G.; Stevenson, D. M.; Chu, F. S. T.; Cleland, W. W.; Weimer, P. J.; Currie, C. R. *Science* **2009**, *326*, 1120−1123.
(18) Anthraper, A.; DuBois, J. D. *Am. J. Bot.* **2003**, *90*, 683−692.
(19) Hara, S.; Hashidoko, Y.; Desyatkin, R. V.; Hatano, R.; Tahara, S. *Appl. Environ. Microb* **2009**, *75*, 2811−2819.
(20) Schöllhorn, R.; Burris, R. H. *Proc. Natl. Acad. Sci. U. S. A.* **1967**, *58*, 213−216.
(21) Hardy, R. W.; Holsten, R.; Jackson, E.; Burns, R. *Plant Physiol.* **1968**, *43*, 1185−1207.
(22) Mårtensson, A.; Ljunggren, H. *Plant Soil* **1984**, *81*, 177−184.
(23) Minchin, F. R.; Witty, J. F.; Sheehy, J. E.; Muller, M. *J. Exp. Bot.* **1983**, *34*, 641−649.
(24) Hardy, R. W. F.; Burns, R. C.; Holsten, R. D. *Soil Biol. Biochem.* **1973**, *5*, 47−81.
(25) Seitzinger, S. P.; Garber, J. H. *Mar. Ecol.: Prog. Ser.* **1987**, *37*, 65−73.
(26) Bellenger, J.; Xu, Y.; Zhang, X.; Morel, F.; Kraepiel, A. *Soil Biol. Biochem.* **2014**, *69*, 413−420.
(27) Weber, A. *Raman Spectroscopy of Gases and Liquids*; Springer Science and Business Media: Berlin, Heidelberg, Germany, 2012; Vol. *11*.
(28) Peoples, M.; Herridge, D.; Ladha, J. *Plant Soil* **1995**, *174*, 3−28.
(29) Carlsson, G.; Huss-Danell, K. *Plant Soil* **2003**, *253*, 353−372.
(30) Hoagland, D. R.; Arnon, D. I. *The Water-Culture Method for Growing Plants without Soil*: Agricultural Experiment Station: Berkley, CA, 1950; Vol. *347*.
(31) Pereyra, G.; Hartmann, H.; Michalzik, B.; Ziegler, W.; Trumbore, S. *Forests* **2015**, *6*, 3686−3703.
(32) Phillips, D. A.; Newell, K. D.; Hassell, S. A.; Felling, C. E. *Am. J. Bot.* **1976**, *63*, 356−362.
(33) Cabrerizo, P. M.; Gonzalez, E. M.; Aparicio-Tejo, P. M.; Arrese-Igor, C. *Physiol. Plant.* **2001**, *113*, 33−40.
(34) Fischinger, S. A.; Hristozkova, M.; Mainassara, Z. A.; Schulze, J. *J. Exp. Bot.* **2010**, *61*, 121−130.
(35) Cardenas, L. M.; Hawkins, J. M. B.; Chadwick, D.; Scholefield, D. *Soil Biol. Biochem.* **2003**, *35*, 867−870.
(36) Wang, R.; Willibald, G.; Feng, Q.; Zheng, X.; Liao, T.; Brüggemann, N.; Butterbach-Bahl, K. *Environ. Sci. Technol.* **2011**, *45*, 6066−6072.
(37) Jochum, T.; Michalzik, B.; Bachmann, A.; Popp, J.; Frosch, T. *Analyst* **2015**, *140*, 3143−3149.
(38) Keiner, R.; Herrmann, M.; Kuesel, K.; Popp, J.; Frosch, T. *Anal. Chim. Acta* **2015**, *864*, 39−47.
(39) Keiner, R.; Frosch, T.; Massad, T.; Trumbore, S.; Popp, J. *Analyst* **2014**, *139*, 3879−3884.
(40) Frosch, T.; Popp, J. *J. Mol. Struct.* **2009**, *924*−*926*, 301−308.
(41) Frosch, T.; Popp, J. *J. Biomed. Opt.* **2010**, *15*, 041516.
(42) Salter, R.; Chu, J.; Hippler, M. *Analyst* **2012**, *137*, 4669−4676.
(43) Kiefer, J.; Seeger, T.; Steuer, S.; Schorsch, S.; Weikl, M.; Leipertz, A. *Meas. Sci. Technol.* **2008**, *19*, 085408.
(44) Keiner, R.; Gruselle, M. C.; Michalzik, B.; Popp, J.; Frosch, T. *Anal. Bioanal. Chem.* **2015**, *407*, 1813−1817.
(45) Jochum, T.; Rahal, L.; Suckert, R. J.; Popp, J.; Frosch, T. *Analyst* **2016**, *141*, 2023−2029.
(46) Frosch, T.; Keiner, R.; Michalzik, B.; Fischer, B.; Popp, J. *Anal. Chem.* **2013**, *85*, 1295−1299.
(47) Jochum, T.; von Fischer, J. C.; Trumbore, S.; Popp, J.; Frosch, T. *Anal. Chem.* **2015**, *87*, 11137−11142.
(48) Keiner, R.; Frosch, T.; Hanf, S.; Rusznyak, A.; Akob, D. M.; Kusel, K.; Popp, J. *Anal. Chem.* **2013**, *85*, 8708−8714.
(49) King, D. A.; Pittaro, R. J. *Opt. Lett.* **1998**, *23*, 774−776.
(50) Beebe, K. R.; Pell, R. J.; Seasholtz, M. B. *Chemometrics: A Practical Guide*; Wiley-Interscience: New York, 1998; Vol. *4*.
(51) Le, L. D.; Tate, J. D.; Seasholtz, M. B.; Gupta, M.; Owano, T.; Baer, D.; Knittel, T.; Cowie, A.; Zhu, J. *Appl. Spectrosc.* **2008**, *62*, 59−65.
(52) Yaws, C. L. *The Yaws Handbook of Vapor Pressure: Antoine Coefficients*; Gulf Professional Publishing: Oxford, U.K., 2015.
(53) Vance, C. P.; Heichel, G. H. *Annu. Rev. Plant Physiol. Plant Mol. Biol.* **1991**, *42*, 373−392.
(54) Herridge, D. F.; Pate, J. S. *Plant Physiol.* **1977**, *60*, 759−764.
(55) Ryle, G. J. A.; Powell, C. E.; Gordon, A. J. *J. Exp. Bot.* **1985**, *36*, 634−643.
(56) Vance, C. P.; Stade, S.; Maxwell, C. A. *Plant Physiol.* **1983**, *72*, 469−473.
(57) Schulze, J. *J. Plant Nutr. Soil Sci.* **2004**, *167*, 125−137.
(58) Schulze, J.; Temple, G.; Temple, S. J.; Beschow, H.; Vance, C. P. *Ann. Bot.* **2006**, *98*, 731−740.
(59) Fischinger, S. A.; Schulze, J. *J. Exp. Bot.* **2010**, *61*, 2281−2291.
(60) Thorstensen, J.; Haugholt, K. H.; Ferber, A.; Bakke, K. A. H.; Tschudi, J. *J. Eur. Opt. Soc. - Rapid Publ.* **2014**, *9*, 14054.

DOI: 10.1021/acs.analchem.6b03101
Anal. Chem. 2017, 89, 1117−1122